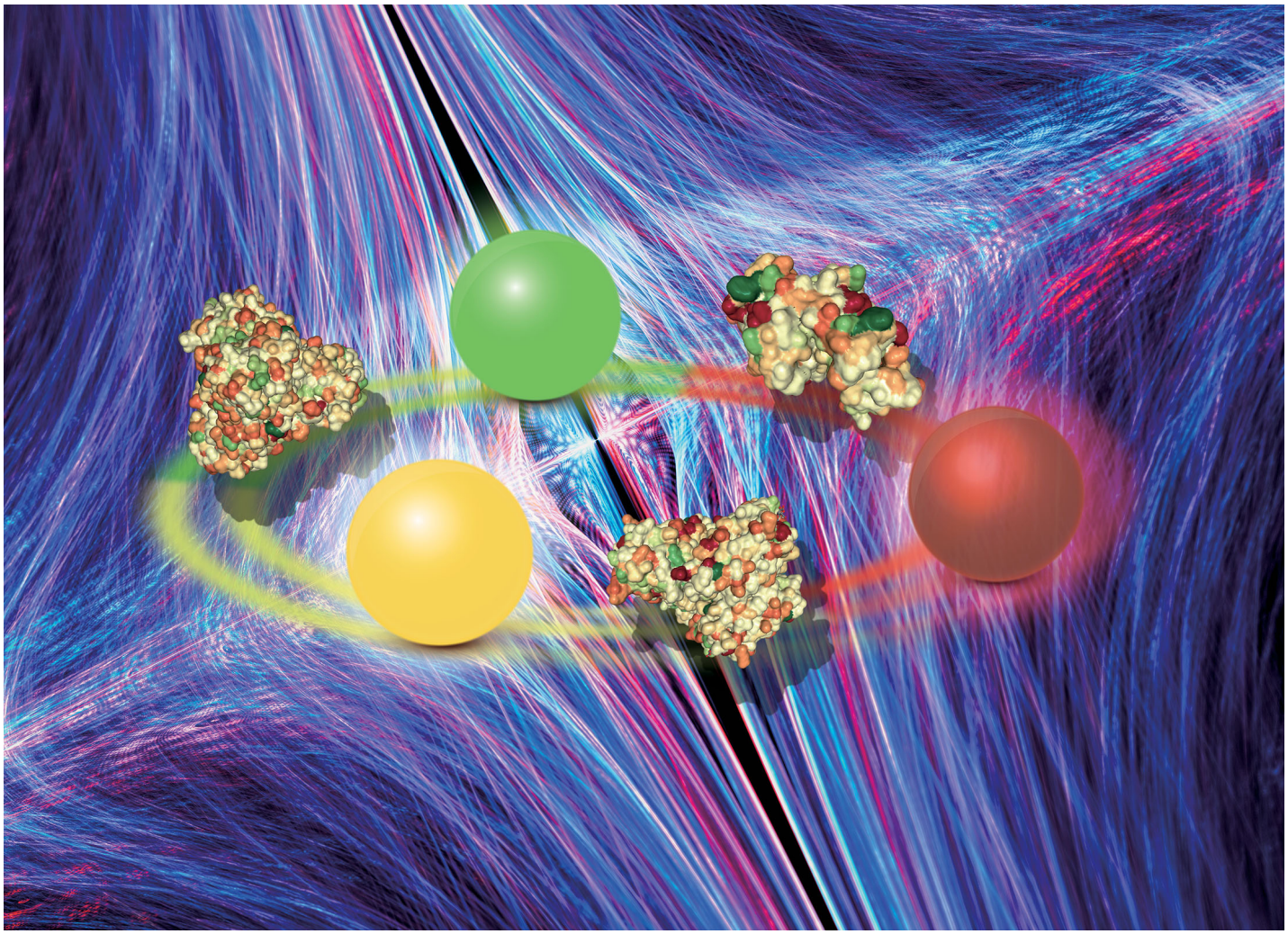

**Showcasing research from Professor Weili Wei's laboratory, School of Pharmaceutical Sciences, Chongqing University in China. Image was designed and illustrated by Xu Jie.**

Simultaneous quadruple-channel optical transduction of a nanosensor for multiplexed qualitative and quantitative analysis of lectins

An optical nanosensor capable of identifying and quantitating multiple lectins simultaneously was developed. The quadruple channel of fluorescence and scattering signals can be *in situ* collected from the same solution system, which offers high accuracy, discrimination resolution and measurement convenience.

## As featured in:


See Weili Wei *et al.*, *Chem. Commun.*, 2018, **54**, 7754.

ROYAL SOCIETY OF CHEMISTRY

rsc.li/chemcomm

Registered charity number: 207890

ChemComm

COMMUNICATION

View Article Online
View Journal | View Issue



Cite this: *Chem. Commun.*, 2018, **54**, 7754

Received 16th March 2018,
Accepted 17th May 2018

DOI: 10.1039/c8cc02138d

rsc.li/chemcomm



# Simultaneous quadruple-channel optical transduction of a nanosensor for multiplexed qualitative and quantitative analysis of lectins†

Lu Wang, Yue Zhang, Hui He, Haimei Yang and Weili Wei *

**A multichannel optical nanosensor capable of identifying and quantitating multiple lectins simultaneously was developed. The quadruple channel of fluorescence and scattering signals can be *in situ* collected from the same solution system, which offers high accuracy, discrimination resolution and measurement convenience. This nanosensor can in principle be generalized to the analysis of all lectins and saccharide binding organisms.**

A lectin is a saccharide-binding protein or glycoprotein of non-immune origin which agglutinates cells and/or precipitates glycoconjugates present in animals, plants and microbes.[1–3] The specific interactions between lectins and saccharides involve various physiological and pathological processes, such as inflammatory responses,[4] cell–cell interaction and cancer metastasis.[5] Therefore, the qualitative and quantitative analysis of lectins plays an integral role in understanding and exploring important biological behaviors. The previously reported methods based on fluorometry,[6] colorimetry,[7] and electrochemistry[8] are usually time-consuming, laborious, and error-prone. In addition, most of these methods are aimed at one specific lectin, for instance, concanavalin A (Con A),[9,10] which is hard to meet the practical needs, in light of the fact that even an immune reaction or a disease is often involved with a wide variety of lectins.[11,12] Hence, there is an urgent need to develop general and facile methods which detect multiple lectins simultaneously.

In recent years, array sensors that simulate human olfaction to carry out analysis have been widely used for multiplexed analysis. These sensors follow a hypothesis-free signature-based strategy[13] that allows them to be "trained" to identify diverse bioanalytes (*i.e.* proteins) in research areas of environmental science, clinical diagnosis, drug discovery, chemical engineering and food industry.[14,15] However, due to the limited recognition elements in comparison with the olfactory system, the discrimination ability of traditional array sensors is deficient. Furthermore, the single-channel output of these sensors requires separate measurements for each array element, which hampers convenience and accuracy.

Multidimensional array sensors with more than one signal transduction channel offer improved discrimination accuracy and/or diversity. Nevertheless, the majority of them only extract duel-[16] or triple-[17] channel information, and extraordinary rare examples extracting quadruple-channel signals suffer from inter-channel signal interference,[18] or an inconvenient multistep sample process.[19,20] It is still a challenge to extract *in situ* four or even more pieces of dimensional information from a single sample system. The recognition and quantitation of lectins based on multichannel sensors has not been reported so far.

Herein, we introduced a saccharide-lectin recognition-based quadruple-channel nanosensor by using fluorescence resonance energy transfer (FRET) and Rayleigh resonance scattering (RRS) as signal transduction principles for general analysis of multiple lectins. As we all know, fluorescence detection possesses very high sensitivity and has been widely used for bioimaging.[21–23] Thus, in the present work the FRET and RRS signal-based quadruple-channel nanosensor would be used to analyse lectins with a very low limit of detection. Moreover, the simultaneous quadruple-channel optical transduction provides a ratiometric output that enhances the accuracy of the measurements. Finally, the nanosensor only responds to lectins and excludes all the other numerous non-saccharide binding proteins, which is beneficial for practical applications. As shown in Scheme 1, the intelligence system was established using six kinds saccharide functionalized multicolor emitting CdSe/ZnS quantum dots (QDs). Specifically, green emitting QDs (G-QDs) with maximal emission at 518 nm were modified with mannose (Man-G-QDs) and *N*-acetylglucosamine (GlcNac-G-QDs) respectively; yellow emitting QDs (Y-QDs) with maximal emission at 582 nm were modified with galactose (Gal-Y-QDs) and *N*-acetyl glucosamine (GlcNac-Y-QDs) respectively; and the red emitting QDs with maximal emission at 659 nm (R-QDs) were modified with mannose (Man-R-QDs) and galactose (Gal-R-QDs) respectively. G-QDs, Y-QDs and R-QDs are robust inorganic chromophores

*School of Pharmaceutical Sciences, Chongqing University, Chongqing 401331, P. R. China. E-mail: wlwei@cqu.edu.cn*

† Electronic supplementary information (ESI) available. See DOI: 10.1039/c8cc02138d

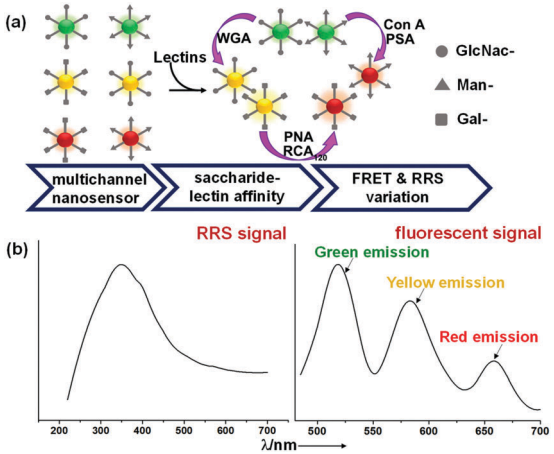


Scheme 1 (a) Schematic illustration of the multichannel nanosensor for the identification of lectins and (b) the quadruple-channel signal including one RRS and three fluorescence emission ($\lambda_{ex}$ = 360 nm) signals.

that provide excitation spectra of longer wavelength emitting QDs overlapping with the emission spectra of shorter wavelength emitting QDs (Fig. S1, ESI†), and thus allowing FRET when they are close enough. In the presence of target lectins, they specifically bind to certain saccharide-modified QDs. We chose 360 nm as the excitation wavelength to reach a compromise of emission intensity and anti-interference of second-order scattering of the excitation light (Fig. S2, ESI†). The multivalent interaction of lectins with saccharide moieties results in agglutination of certain QDs. The aggregation allows the distances between specific QDs to decrease and leads to FRET, providing a platform for optical probes to perform target detection. Whilst QDs are scattering particles that bring in RRS in the same incident light, the RRS intensity can be greatly increased upon particle aggregation.[24–26] In a word, these glycosylated QDs serve as energy donor–acceptor pairs of FRET and scattering particles. Their corresponding fluorescence and RRS signals based on target-induced aggregation of nanoparticles are attractive for sensing. Moreover, the multichannel signals can be monitored *in situ* with the same equipment, endowing the nanosensor with the capability of simultaneous identification and quantitation of lectins *via* statistical analysis.

The lectin recognizable saccharides D-mannopyranose (Man), D-galactopyranose (Gal) and D-*N*-acetyl glucosamine (GlcNac) were first thiolated and then grafted onto the surface of QDs *via* the formation of metal–sulfur bonds. According to previous reports,[27,28] the Man, Gal and GlcNac were thiolated to 3-mercaptopropyl glycosides, which were named as Man-SH, Gal-SH and GlcNac-SH, respectively. The details of the synthesis are shown in the ESI.†

The glycosylated QDs were prepared *via* phase transfer reactions between a chloroform phase and an aqueous phase.[29] The commercially as-received QDs were capped with hydrophobic octylamine and dispersible in $CHCl_3$. As a result, ligand exchange of hydrophobic octylamine on QDs with Man-SH, Gal-SH and GlcNac-SH was carried out, respectively. Typically, 1 mg QDs dispersed in 1 mL chloroform and 20 mg thiolated saccharides dissolved in 10 mL water were mixed. Then, the mixture was stirred violently at room temperature until QDs were collected and purified *via* dialysis for 2 days for subsequent experiments. The chemical composition of the QDs before and after the mixing process was fully transferred from the chloroform phase in the bottom to the upper aqueous layer. The upper aqueous layer being modified with three different saccharides was examined using Fourier transform infrared (FT-IR) spectroscopy. The three peaks that appeared at 1159, 1217 and 1121 $cm^{-1}$ in the corresponding FT-IR spectra could be ascribed to the C–O–C stretching vibrations, which are unique characteristics of saccharide moieties (Fig. S3–S5, ESI†). In addition, the morphologies of saccharide-modified G-, Y-, and R-QDs were investigated using transmission electron microscopy (Fig. S6, ESI†). The QDs remained spherical and mono-dispersible in water.

Subsequently, the quadruple-channel nanosensor was established by mixing the six kinds of QDs (Man-G-QDs, GlcNac-G-QDs, Gal-Y-QDs, GlcNac-Y-QDs, Man-R-QDs and Gal-R-QDs) with the same weight concentration in aqueous solution to a total concentration of 50 μg $mL^{-1}$. As a proof-of-concept system, we chose five lectins (Table 1) and two non-saccharide binding proteins that have diverse properties (*i.e.* molecular weight, number of subunits and binding specificity) as the sensing analytes. Take the four-valent Con A, a Man-binding lectin, for example, it led to FRET between Man-G-QDs and Man-R-QDs, which brought fluorescence intensity changes, and aggregation of Man-G-QDs and Man-R-QDs which contributed to the RRS signal enhancement. The intensities of the fluorescence emission at 518 nm, 582 nm and 659 nm and RRS at 338 nm were recorded before and after adding different lectins. Fig. 1 shows the fluorescence and RRS signals induced by five lectins (1 μM), including Con A, wheat germ agglutinin (WGA), peanut agglutinin (PNA), *Ricinus communis* agglutinin ($RCA_{120}$) and *Pisum sativum* agglutinin (PSA). Accordingly, different lectins resulted in distinct distinguishable quadruple-channel signals due to their different binding constants with different saccharide moieties (Table S1, ESI†). Due to the different binding behaviors of the lectins, the FRET efficiencies were measured to be different (Table S2, ESI†) in the presence of 1 μM lectins according to a previously reported calculation method.[30]

Next, we further explored the ability of the nanosensor for the identification of the model lectins including Con A, WGA, PNA, $RCA_{120}$ and PSA. Afterwards, 50 μL of lectin (1 μM final concentration) was added to 30 μL of (5 μg $mL^{-1}$ final concentration) the nanosensor solution. Subsequently, the mixture was diluted with phosphate buffered saline (PBS, 20 mM, pH 7.4) containing 0.1 mM $MnCl_2$, 0.1 mM $MgCl_2$, and 0.1 mM $CaCl_2$[31] to a final volume of 300 μL. After incubating at room temperature (25 °C) for 2 h, the mixture was transferred into a 360 μL quartz cuvette carefully to measure the fluorescence at a single excitation wavelength of 360 nm and RRS spectra with the same excitation wavelength. With the fluorescence

Table 1 Properties of the five model lectins

| Lectins | $M_w$ (kDa) | No. of subunits | Binding specificity |
|---|---|---|---|
| Con A | 104 | 4 | Man |
| WGA | 36 | 2 | GlcNac |
| PNA | 110 | 4 | Gal |
| $RCA_{120}$ | 120 | 2 | Gal |
| PSA | 53 | 4 | Man |

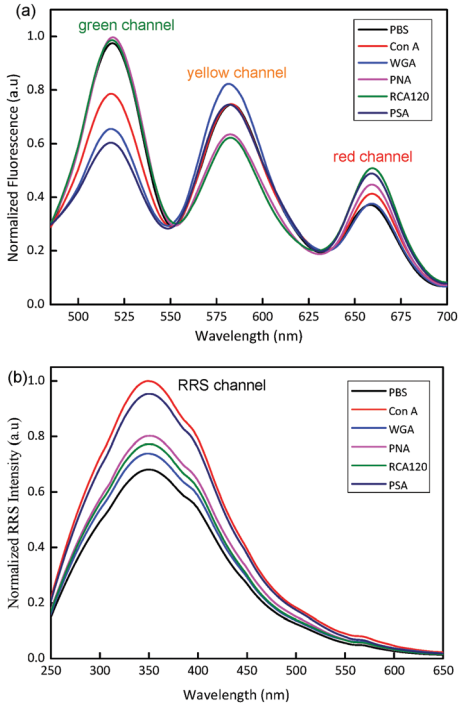


Fig. 1 (a) Emission ($\lambda_{ex}$ = 360 nm) and (b) RRS spectra of the multichannel nanosensor in response to 1 μM Con A, WGA, PNA, $RCA_{120}$, or PSA in comparison with an equal volume of PBS (20 mM, pH 7.4).

and RRS signals recorded, the signal changing rate ($R$) is defined as $(I - I_0)/I_0 \times 100\%$, where $I$ and $I_0$ are the intensity of fluorescence and RRS in the presence and absence of lectins. The multichannel signal changing rates in Fig. 2a and the relative heat map in Fig. 2b indicate that these different signal responses can be used as an optical fingerprint for lectin multiplex recognition using the nanosensor. A canonical score plot for the multichannel signal as obtained from linear discriminant analysis (LDA) was then obtained (Fig. 2c). As shown in Fig. 2c, all target lectins were separated completely from each other, demonstrating that they were effectively discriminated by the multichannel nanosensor. Hierarchical clustering analysis (HCA)

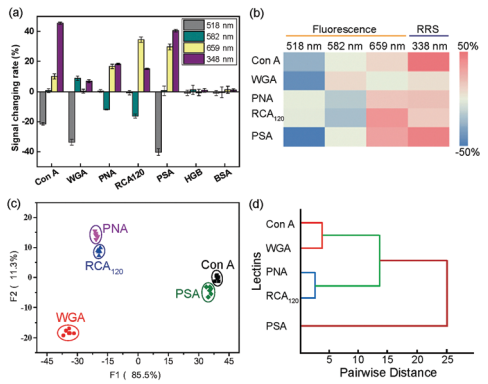


Fig. 2 Statistical analysis of five lectins. (a) Signal patterns obtained by measuring fluorescence and RRS intensity changes at four channels, (b) heat map of the signal patterns for the five lectins, (c) LDA clustering of the lectins *via* LDA of the signal patterns, and (d) HCA of the signal responses producing three distinct clusters.

of the 4-channel signal responses (Fig. 2a) produced three distinct clusters (Fig. 2d), each corresponding to an individual saccharide recognition mechanism, *i.e.* Man, Gal and GlcNac moiety recognition, respectively. Additionally, being non-saccharide binding proteins, both BSA and HGB induced negligible signals (Fig. 2a; Fig. S7, ESI†), revealing the specificity of the nanosensor for lectins only. In brief, the multichannel nanosensor provided methodological feasibility to multiplexed qualitative analysis of lectins.

The multiplexed quantitative analysis of lectins was further carried out with the nanosensor. Because the factor (1) in Fig. 2c is greater than 85%, we simplified it by using factor (1) to quantify the lectins.[32] As shown in Fig. 3, we applied this multichannel nanosensor for detecting lectins at sub-μM concentrations. The linearity of the dose–response curves in Fig. 3b reveals that the concentration-dependent signal changing rate can be used for Con A quantitation. The limit of detection (LOD) is calculated by $3\sigma/S$, where $\sigma$ and $S$ are the standard deviation of the noise at zero concentration and the slope of the fitted curve. The LOD of Con A was calculated to be 4.9 nM. Moreover, the quantitative analysis of WGA, PNA, $RCA_{120}$ and PSA based on this multichannel nanosensor was also performed satisfactorily (Fig. S8–S11, ESI†) with LODs of 9.7 nM, 8.9 nM, 5.7 nM and 4.6 nM, respectively. Significantly, the sensor can still get an obvious signal with 10 nM lectins (Fig. S12, ESI†). As multiplexed sensing for proteins has become increasingly important for precise disease diagnosis,[33–35] we further verified the real sample analysis capability of the nanosensor by using human

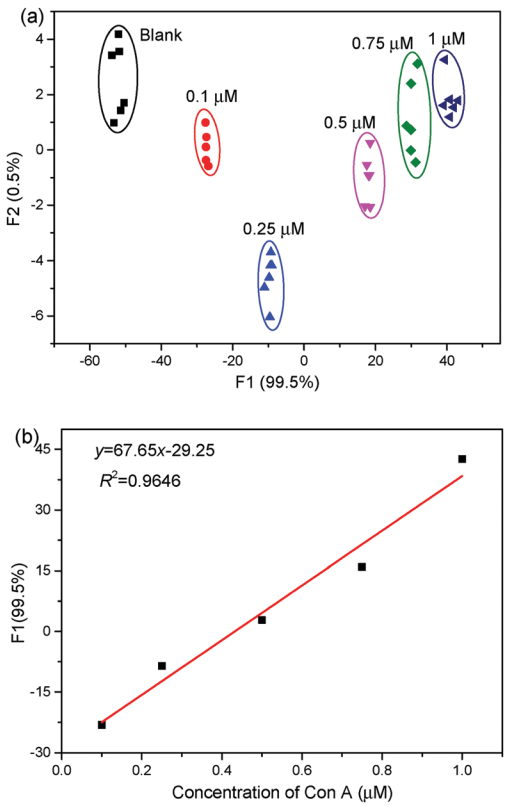


Fig. 3 Quantitative analysis of Con A. (a) LDA score plot of Con A with concentrations of 0, 0.1, 0.25, 0.5, 0.75, and 1.0 μM. (b) Liner fitting between factor (1) and Con A.

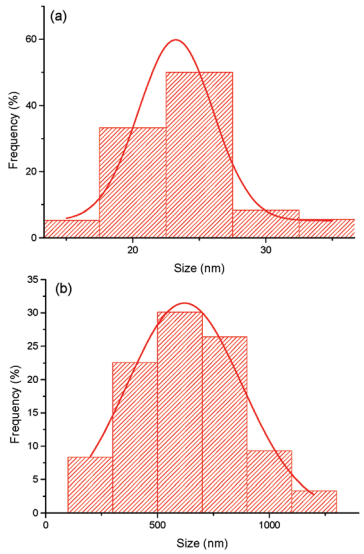


Fig. 4 The hydrodynamic size distribution of the nanosensor in the (a) absence and (b) presence of Con A (1 μM).

serum as the matrix. As shown in Tables S3–S7 (ESI†), the quantitative accuracy for each lectin in human serum was satisfactory.

The simultaneous identification and quantitation of multiple lectins based on the quadruple-channel optical nanosensor constructed with glycosylated QDs has been verified. The underlying mechanisms should be due to differential association and/or aggregation between the QDs induced by different lectins, which resulted in differential fluorescence and RRS signal patterns. For instance, upon the addition of Con A to the nanosensor solution system, the average hydrodynamic diameters of scattering particles increased from *ca.* 24 to *ca.* 611 nm according to the dynamic light scattering (DLS) measurements (Fig. 4). Obviously, the change was induced by the formation of aggregates in the presence of the target lectin. These observations support our hypothesis that the fluorescence and RRS intensity changes in the presence of lectins are indeed ascribed to the formation of agglutinations.

In summary, we have designed and built a novel multichannel optical nanosensor based on six kinds of glycosylated fluorescent QDs with green, yellow and red emission. This nanosensor can transduce simultaneously quadruple-channel optical signals including fluorescence and RRS, which is beneficial for facile and accurate signal collection using a simple fluorescence spectrophotometer. The nanosensor is specific to lectins with negligible interference from any other non-saccharide binding proteins. The information-rich outputs allow accurate, sensitive, and multiplexed identification and quantitation of lectins. This nanosensor should also be suitable for the detection of human pathogens that possess multiple lectins on their surface. The simplicity and effectiveness of the system provides a potential way forward for clinical diagnosis, antibiotic discovery, and therapeutic monitoring.

Financial support was provided by the National Natural Science Foundation of China (No. 21675016), the Chongqing Basic and Frontier Research Program (No. cstc2016jcyjA0328), and the 100 Young Plan by Chongqing University (No. 0236011104410).

## Conflicts of interest

There are no conflicts to declare.

## Notes and references

1 I. J. Goldstein, R. C. Hughes, M. Monsigny, T. Osawa and N. Sharon, *Nature*, 1980, **285**, 66.
2 Y. Belkaid and O. J. Harrison, *Immunity*, 2017, **46**, 562–576.
3 Y. Belkaid and T. W. Hand, *Cell*, 2014, **157**, 121–141.
4 O. Takeuchi and S. Akira, *Cell*, 2010, **140**, 805–820.
5 G. I. Bell, *Science*, 1978, **200**, 618–627.
6 Q. Chen, W. Wei and J.-M. Lin, *Biosens. Bioelectron.*, 2011, **26**, 4497–4502.
7 X.-L. Hu, H.-Y. Jin, X.-P. He, T.-D. James, G.-R. Chen and Y.-T. Long, *ACS Appl. Mater. Interfaces*, 2015, **7**, 1874–1878.
8 X. Li, Y. Wang, L. Shi, H. Ma, Y. Zhang, B. Du, D. Wu and Q. Wei, *Biosens. Bioelectron.*, 2017, **96**, 113–120.
9 X. Ma, J. Li, Y. Liu, Y. Yuan and G. Xu, *Sens. Actuators, B*, 2017, **248**, 201–206.
10 F. Hu, S. Chen, C. Wang, R. Yuan, Y. Xiang and C. Wang, *Biosens. Bioelectron.*, 2012, **34**, 202–207.
11 G. A. Rabinovich and M. A. Toscano, *Nat. Rev. Immunol.*, 2009, **9**, 338–352.
12 I. M. Dambuza and G. D. Brown, *Curr. Opin. Immunol.*, 2015, **32**, 21–27.
13 K. J. Albert, N. S. Lewis, C. L. Schauer, G. A. Sotzing, S. E. Stitzel, T. P. Vaid and D. R. Walt, *Chem. Rev.*, 2000, **100**, 2595–2626.
14 M. P. Landry, H. Ando, A. Y. Chen, J. C. Cao, V. I. Kottadiel, L. Chio, D. Yang, J. Y. Dong, T. K. Lu and M. S. Strano, *Nat. Nanotechnol.*, 2017, **12**, 368–377.
15 Y. Lu, H. Kong, F. Wen, S. Zhang and X. Zhang, *Chem. Commun.*, 2013, **49**, 81–83.
16 J. Hu, X. M. Jiang, L. Wu, K. L. Xu, X. D. Hou and Y. Lv, *Anal. Chem.*, 2011, **83**, 6552–6558.
17 S. Rana, N. D. B. Le, R. Mout, K. Saha, G. Y. Tonga, R. E. S. Bain, O. R. Miranda, C. M. Rotello and V. M. Rotello, *Nat. Nanotechnol.*, 2015, **10**, 65–69.
18 W. Huang, Z. Y. Xie, Y. Q. Deng and Y. He, *Sens. Actuators, B*, 2018, **254**, 1057–1060.
19 C. Li, P. Wu and X. Hou, *Nanoscale*, 2016, **8**, 4291–4298.
20 M. Schmittel and H. W. Lin, *Angew. Chem., Int. Ed.*, 2007, **46**, 893–896.
21 W. Chen, S. Xu, J. J. Day, D. Wang and M. Xian, *Angew. Chem., Int. Ed.*, 2017, **56**, 16611–16615.
22 K. Xu, D. Luan, X. Wang, B. Hu, X. Liu, F. Kong and B. Tang, *Angew. Chem., Int. Ed.*, 2016, **55**, 12751–12754.
23 W. Chen, A. Pacheco, Y. Takano, J. J. Day, K. Hanaoka and M. Xian, *Angew. Chem., Int. Ed.*, 2016, **55**, 9993–9996.
24 Y. Li, J. Chen, S. Zhuo, Y. Wu, C. Zhu and L. Wang, *Microchim. Acta*, 2004, **146**, 13–19.
25 X. Chen, Y. Dong, L. Fan, D. Yang and M. Zhang, *Anal. Chim. Acta*, 2007, **597**, 300–305.
26 M. Rabiee, A. R. Mirhabibi, F. M. Zadeh, R. Aghababazadeh, E. M. Pour and L. Lin, *Pigm. Resin Technol.*, 2008, **37**, 224–228.
27 B. T. Houseman, E. S. Gawalt and M. Mrksich, *Langmuir*, 2003, **19**, 1522–1531.
28 M. Hartmann, P. Betz, Y. C. Sun, S. N. Gorb, T. K. Lindhorst and A. Krueger, *Chem. – Eur. J.*, 2012, **18**, 6485–6492.
29 Y. Yang, Y. T. Zhao, T. T. Yan, M. Yu, Y. L. Sha, Z. H. Zhao and Z. J. Li, *Tetrahedron Lett.*, 2010, **51**, 4182–4185.
30 Q. Li and S. Seeger, *J. Phys. Chem. B*, 2011, **115**, 13643–13649.
31 H. Zhang, L. Zhang, R.-P. Liang, J. Huang and J.-D. Qiu, *Anal. Chem.*, 2013, **85**, 10969–10976.
32 F. Zhang, C. Lu, M. Wang, X. Yu, W. Wei and Z. Xia, *ACS Sens.*, 2018, **3**, 304–312.
33 X.-P. He, X.-L. Hu, T. D. James, J. Yoon and H. Tian, *Chem. Soc. Rev.*, 2017, **46**, 6687–6696.
34 J.-X. Song, X.-Y. Tang, D.-M. Zhou, W. Zhang, T. D. James, X.-P. He and H. Tian, *Mater. Horiz.*, 2017, **4**, 431–436.
35 D.-K. Ji, G.-R. Chen, X.-P. He and H. Tian, *Adv. Funct. Mater.*, 2015, **25**, 3483–3487.